CONF-9210315--4

PREPARED FOR THE U.S. DEPARTMENT OF ENERGY,
UNDER CONTRACT DE-AC02-76-CHO-3073

PPPL-2896
UC-420,426

PPPL-2896

ACHIEVING HIGH FUSION REACTIVITY IN HIGH POLOIDAL BETA DISCHARGES IN TFTR

BY

M.E. MAUEL, G.A. NAVRATIL, S.A. SABBAGH, S. BATHA, ET AL.

APRIL, 1993

PPPL PRINCETON PLASMA PHYSICS LABORATORY

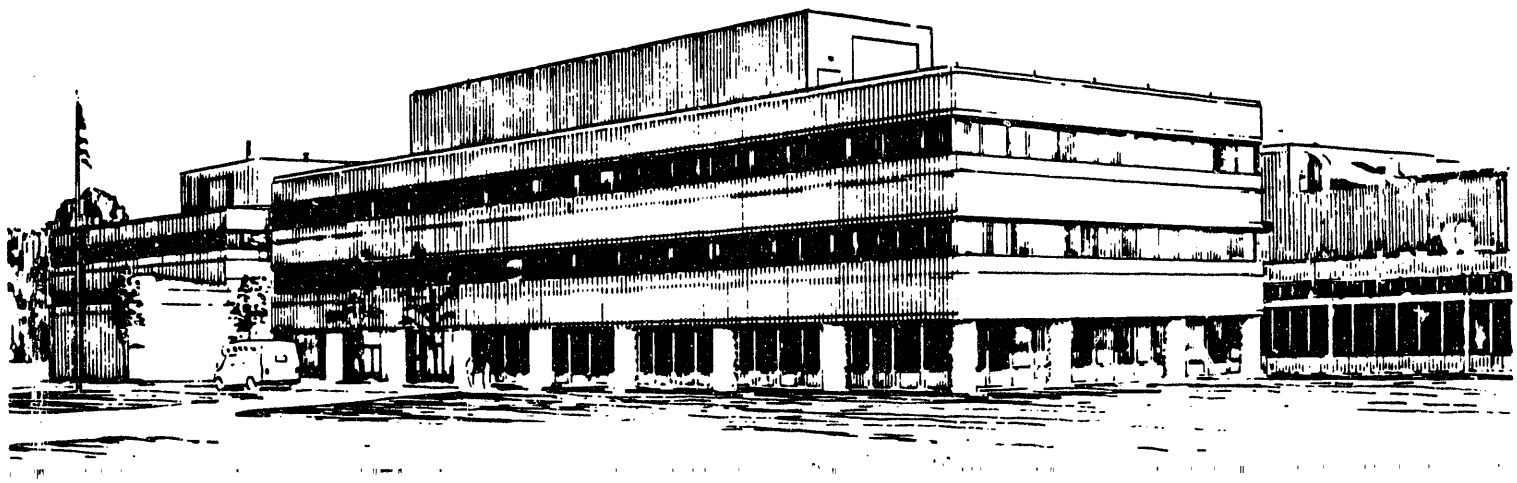

NOTICE

This is a preprint of a paper presented at the Fourteenth International Conference on Plasma Physics and Controlled Nuclear Fusion Research, September 30 through October 7, 1992 in Wurzburg, Germany.

INTERNATIONAL ATOMIC ENERGY AGENCY

FOURTEENTH INTERNATIONAL CONFERENCE ON PLASMA PHYSICS AND CONTROLLED NUCLEAR FUSION RESEARCH

Würzburg, Germany, 30 September – 7 October 1992

IAEA-CN-56/ A-III-4

Achieving High Fusion Reactivity in High Poloidal Beta Discharges in TFTR*

M. E. MAUEL, G. A. NAVRATIL, S. A. SABBAGH
Department of Applied Physics
Columbia Univeristy
New York, New York

S. BATHA, M. G. BELL, R. BELL, R. V. BUDNY, C. E. BUSH, A. CAVALLO, M. S. CHANCE, C. Z. CHENG, P. C. EFTHIMION, E. D. FREDRICKSON, G. Y. FU, R. J. HAWRYLUK, A. C. JANOS, D. L. JASSBY, F. LEVINTON, D. R. MIKKELSEN, J. MANICKAM, D. C. MCCUNE, K. M. MCGUIRE, S. S. MEDLEY, D. MUELLER, Y. NAGAYAMA, D. K. OWENS, H. K. PARK, A. T. RAMSEY, B. C. STRATTON, E. J. SYNAKOWSKI, G. TAYLOR, R. M. WIELAND, M. YAMADA, M. C. ZARNSTORFF, AND S. ZWEBEN
Princeton Plasma Physics Laboratory
Princeton Univeristy
Princeton, New Jersey

J. KESNER, E. MARMAR, J. SNIPES, J. TERRY
Plasma Fusion Center
Massachusetts Institute of Technology
Cambridge, Massachusetts

United States of America

* Supported by US Department of Energy contracts DE-FG02-89ER53297, DE-AC02-76-CHO-3073, and DE-FG02-90ER54084

Abstract

ACHIEVING HIGH FUSION REACTIVITY IN HIGH POLOIDAL BETA DISCHARGES IN TFTR.

High poloidal beta discharges have been produced in TFTR that achieved high fusion reactivities at low plasma currents. By rapidly decreasing the plasma current just prior to high-power neutral beam injection, relatively peaked current profiles were created having high $l_i > 2$, high Troyon-normalized beta, $\beta_N > 3$, and high poloidal beta, $\beta_p \geq 0.7\ R/a$. The global energy confinement time after the current ramp was comparable to supershots, and the combination of improved MHD stability and good confinement produced a new high $\varepsilon\beta_p$, high Q_{DD} operating mode for TFTR. Without steady-state current profile control, as the pulse lengths of high β_p discharges were extended, l_i decreased, and the improved stability produced immediately after by the current ramp deteriorated. In four second, high $\varepsilon\beta_p$ discharges, the current profile broadened under the influence of bootstrap and beam-drive currents. When the calculated voltage throughout the plasma nearly vanished, MHD instabilities were observed with β_N as low as 1.4. Ideal MHD stability calculations showed this lower beta limit to be consistent with theoretical expectations.

1. Introduction

Tokamak operation at high poloidal beta ($\varepsilon\beta_p \sim 1$, $\varepsilon \equiv a/R$) offers several important advantages to future fusion reactors: low plasma current, high bootstrap current fraction, and the possibility of improved confinement due to equilibrium modification. However, since the plasma current is relatively low at high $\varepsilon\beta_p$, the achievement of high fusion reactivity generally requires operation at a high Troyon-normalized beta, $\beta_N \equiv 10^8 \langle\beta\rangle aB_0 / I_p$, and a high L-mode normalized confinement, $H \equiv \tau_E/\tau_{E,ITERp}$. The previously reported TFTR high poloidal beta experiments have explored this advanced operating regime by making use of a rapid plasma current ramp-down to produce high l_i discharges which have improved MHD stability properties [1,2]. The stability improvement obtained with the rapid I_p ramp-down is significant. At very low current (0.3 MA $< I_p <$ 0.6 MA), neutral beam injection into plasmas prepared with I_p ramps produced high l_i discharges with broad pressure profiles that avoided the macroscopic MHD instabilities limiting supershots to $\varepsilon\beta_p < 0.7$ [3,4]. Diverted discharges with $\varepsilon\beta_p \geq 1.3$ have been produced, and the plasma with highest normalized beta in TFTR ($\beta_N \sim 4.9$) was achieved following a 0.85 MA to 0.4 MA current ramp-down. These very low current discharges illustrated operation at the tokamak's poloidal beta limit [5], and allowed moderate-n ballooning modes to be identified with soft x-ray and ECE fluctuation measurements [6]. High l_i discharges have also been produced with a current ramp in DIII-D [7], and slightly elongated discharges ($\kappa \sim 1.2$) achieving record values of $\beta_N > 6$ when $l_i > 2$ have been recently reported [8].

Although the first high $\varepsilon\beta_p$ discharges in TFTR were produced with $I_p \leq$ 0.85 MA, the current ramp-down technique was used recently to produce high β_p discharges with up to 1.4 MA of plasma current. High l_i, high $\varepsilon\beta_p$ discharges achieved $\beta_N \sim 3.5$ at 1.0 MA; whereas, MHD instabilities restrict supershots to operate below $\beta_N < 2.5$. Since fusion reactivity scales roughly as the square of the stored energy in TFTR, this 40% improvement of the beta limit produces a two-fold increase in the fusion reactivity for a given value of plasma current. Figure 1a illustrates this result by showing the peak neutron rates obtained both when using the I_p ramp-down technique and during supershot operation. The higher neutron rate observed below 1.4 MA is a direct result of the improved MHD stability of the transiently-modified current profile.

The high l_i, high $\varepsilon\beta_p$ discharges also achieved high Q_{DD} (the ratio of fusion power to applied power) since discharges with $I_p >$ 0.85 MA have global energy confinement comparable to that obtained in typical supershots

[9]. For high $\varepsilon\beta_p$ plasmas with currents between 1.0 MA and 1.2 MA, the global energy confinement times were between 0.12 s < τ_E < 0.16 s. Q_{DD} as high as 1.3×10^{-3} was measured at 1.0 MA and $\varepsilon\beta_p \sim 0.95$. For lower currents (≤ 0.85 MA), the global energy confinement decreased in a manner consistent with ITER-89P L-mode scaling [10] (*i.e.* $\tau_E \propto I_p^{0.85}$). When the ratio between the pre-ramp and post-ramp current levels was greater than 1.5 and when the neutral beam power was large enough to produce $\varepsilon\beta_p \sim 1$, the L-mode normalized global energy confinement time, H, was found to be between 2.5 and 3.7.

Figure 1b illustrates TFTR's two high Q_{DD} operating regimes as a function of $\varepsilon\beta_p$ and q^* where $q^* \equiv 5a^2B_0\kappa/R^*I_p$ and $R^* \approx R\,2\kappa/(1+\kappa^2)$. High Q_{DD} supershots can be produced in plasmas with 1.2 MA < I_p < 1.9 MA ($3.5 \le q^* \le 5$) provided the injected balanced neutral beam power increases with increasing current. As described elsewhere [4,11], supershot operation is limited by the presence of sawteeth and associated confinement degradation at high current and by pressure-driven MHD instabilities at low current. TFTR's high β_p, high Q_{DD} operating region occurs between 1.0 MA < I_p < 1.2 MA ($5 \le q^* \le 6$) when high power NBI (approximately 25 MW) is applied immediately after a rapid I_p ramp-down. This regime is referred to as the high β_p operating regime. Because of the existence of these two operating modes, future DT experiments in TFTR can study collective alpha-particle physics in discharges having high $\varepsilon\beta_p$, high β_N, and evolving current profiles.

The tendency for high l_i, peaked current profiles to broaden in time also illustrates the need for steady-state current profile control to maintain stable, high Q_{DD} discharges at high $\varepsilon\beta_p$. For $I_p \ge 0.85$ MA, high l_i, high β_N discharges have only been maintained for approximately 0.5 s—equivalent to one alpha-particle slowing-down time—before the onset of beta-limiting disruptions or beta collapses. At lower current, high $\varepsilon\beta_p$ discharges with 0.4 MA ≤ I_p ≤ 0.6 MA have been maintained for more than 2 s by reducing the injected power and β_N. These high $\varepsilon\beta_p$ discharges lasted long enough to allow the current density to relax naturally to a broad profile dominated by beam-driven and bootstrap currents. The magnitude of the non-inductive current was calculated using the TRANSP code [12] to constitute over 90% of the total plasma current. These discharges have enabled TFTR to study the MHD instabilities occurring in long-pulse, high $\varepsilon\beta_p$ plasmas.

2. Achieving high fusion reactivity at high βp

Figure 2 illustrates the time-histories of high $\varepsilon\beta_p$ discharges created using a rapid 1.6 MA to 1.0 MA current ramp. The timing and power level of the neutral beam injection differs slightly for each discharge. In one case, 10 MW of co-injected neutral beam heating was applied during the ramp-down (in order to eliminate sawteeth), and a short 0.3 s, 27 MW pulse of balanced NBI was applied immediately following the I_p ramp. In the other case, 22

MW of balanced NBI was gradually applied so that the peak value of β_N occurred approximately 0.5 s from the end of the current ramp. Both discharges are known to be just below the beta limit since subsequent discharges with slightly higher heating powers disrupted. These four discharges define a time-dependent instability threshold. After 0.3 s from the end of the I_p ramp, the plasma disrupts when $\beta_N \sim 3.5$. After 0.4 s, disruptions occur at $\beta_N \sim 3.1$, and, after 0.5 s, a beta collapse occurred at $\beta_N \sim 2.7$ associated with the presence of intense $m/n = 2/1$ oscillations.

The evolving instability threshold that follows a current ramp is believed to result from the evolution of the plasma current profile. The time history of the internal inductance, $l_i \equiv 4 (\int dV\, B_p^2/2\mu_0) / \mu_0 R^* I_p^2$, (calculated using the TRANSP code for the discharge labeled "a") is a measure of the current evolution. The internal inductance increases from about 1.4 to approximately 2.7 during the I_p ramp and then decreases slowly thereafter.

The observed threshold for MHD instability in supershots occurs at much lower β_N. At 1.4 MA, beta collapses occur for some discharges with $1.3 < \beta_N < 2.1$, and disruptions have occasionally occurred in supershot discharges as low as $\beta_N \sim 1.8$. However, for $\beta_N \geq 2.1$, all 1.4 MA supershots either disrupt or have a beta collapse, and the highest normalized beta achieved for a supershot before the onset of MHD instability is $\beta_N \sim 2.4$.

Figure 3 compares the behaviors of the high l_i, high $\varepsilon\beta_p$ discharges shown in Figure 2 with the time evolution of 1.0 MA and 1.6 MA supershots operating near the supershot beta limit. For each supershot, the power level was adjusted to achieve $\beta_N \sim 2$. Beta collapses with $m/n = 2/1$ occurred for each discharge type, however, one 1.6 MA supershot remained macroscopically stable for a 0.9 s heating pulse. As the figure indicates, the I_p ramp-down increased β_N from 2.0 to 3.5—by a factor approximately equal to the ratio of the initial to the final current levels. Since the plasma's stored energy scales as $\beta_N \times (VI_p / aB)$, the 1.0 MA high l_i discharge and the 1.6 MA supershot have nearly equal plasma energies. (A slightly lower energy resulted for the 1.0 MA high l_i plasma since $\varepsilon\beta_p$ approached unity and its volume, V, was reduced as its cross-section became oblate, $\kappa \sim 0.8$.) When the 1.0 MA high β_p discharge is compared to the 1.0 MA supershot ($\varepsilon\beta_p \sim 0.63$), the increased stability produced by the current ramp allowed the neutron production rate to double.

Figure 4a shows the TRANSP calculated current profiles for the three examples in Figure 3. The rapid current ramp-down creates a current profile with a high central current density and an outer current-reversal layer. The figure also lists the measured values of the density peaking factors, $n_e(0) / \langle n_e \rangle$, and the calculated pressure profile parameters, $\langle p^2 \rangle / \langle p \rangle^2$. The pressure profiles include the calculated pressure of fast beam ions (typically, 40% for supershots and 60% for the I_p ramp-down discharges). The high l_i discharge has a broader density and pressure profile than either supershot; however, the current ramp did not produce profiles as broad as L-mode discharges.

The combination of broad pressure and peaked-current profiles has been shown to produce enhanced stability in TFTR. Figure 4b shows the calculated thresholds for $n = 1$ MHD instability for TFTR discharges having safety factor profiles, $q(\psi)$, representative of either supershots or I_p ramp-downs. For peaked pressure, the stability boundary increases only slightly as l_i increases from 1.0 to 2.5. However, for broad pressure profiles, high l_i discharges are calculated to be stable to $n = 1$ modes for $\beta_N < 5$, and this computed threshold corresponds to the maximum normalized beta achieved in TFTR using a current ramp.

Since current ramps have been used to achieve enhanced confinement in L-mode discharges [6,7,13,14], it is useful to compare the global energy confinement obtained after a current ramp to those obtained with comparable supershots. Figure 3 also shows the approximate values of the global energy confinement times computed both magnetically and with the aid of the TRANSP calculations of l_i. As described in Ref. 9, global τ_E for the two supershots ranged between 0.15 s and 0.17 s; whereas, for the 1.0 MA high $\varepsilon\beta_p$ discharges, global τ_E was in the range of 0.12 s to 0.14 s except during brief periods when each discharge entered a short, ELM-free, limiter H-mode [15,16]. Although many transitions from a supershot to a limiter H-mode have been observed (*e.g.* ELMs are present at the end of the supershot shown in Figure 3a), limiter H-mode transitions are nearly always seen following a current ramp-down in discharges with $I_p \geq 0.85$ MA. Similar behavior following a current ramp-down has been reported in JIPP-T-IIU [17]. The I_p ramp-down shown in Figure 3b resulted in the longest ELM-free period observed in TFTR H-modes, and recent theoretical modeling indicate high l_i current profiles may help stabilize ELMs [18]. When I_p exceeded 1.0 MA, I_p ramps did not produce ELM-free periods, and global energy confinement decreased. Reduced confinement for $I_p > 1.0$ MA prevented high l_i discharges from reaching the beta limit with 28 MW, and fusion reactivity decreased as indicated in Figure 1a. Since the global energy confinement times were nearly equal for the three examples in Figure 3, the confinement multiplier relative to $\tau_{E,ITERp} \propto I_p^{0.85}/\sqrt{P}$ exceeded 3.5 for the high $\varepsilon\beta_p$ discharges. The 1.0 MA supershot had $H \sim 2.8$ while $H \sim 2.5$ for the 1.6 MA supershot.

3. Using high Q_{DD}, high β_p discharges for alpha physics studies

High $\varepsilon\beta_p$ DT discharges have been simulated using the TRANSP code in a manner similar to previously reported DT supershot simulations [19]. These simulations show that Q_{DT} can achieve 0.22 at 1.0 MA using the I_p ramp-down technique, and the values of $Q_{DT}/Q_{DD} \sim 169$ were comparable to supershot ratios. The alpha pressures for high β_p DT plasmas were calculated to be a factor of two lower than the high Q_{DD} supershots, and $\beta_\alpha(0)$ exceeded 0.2% in a 1.2 MA high β_p simulation. The alpha particle slowing-down time

was calculated to be 0.5 s, and this is comparable to the maximum pulse length over which stability can be enhanced with a current ramp. Because the central current density following an I_p ramp-down is nearly equal to the pre-ramp-down current level, prompt alpha losses increased to only 19% at 1.0 MA when compared to an estimated 8% loss for a 1.6 MA supershot.

During the upcoming DT experiments, short heating pulses applied to high l_i plasmas will allow the study of the influence of alpha particles on the stability of high β_p plasmas. Since the DT simulations suggest that the time evolution of global alpha parameters (*e.g.* $\langle\beta_\alpha\rangle$ and V_α/V_A) span a similiar range in both supershot and ramp-down discharges, alpha stability experiments can be made with a variety of $q(\psi)$ profiles and with $\varepsilon\beta_p$ up to unity. We are particularly interested in the stabilizing effects of (1) high normalized pressure gradients, $\alpha \equiv -(2Rq^2 / B^2)(dp/dr)$, which occur at high β_p and may stabilize high-n, TAE modes [20] and (2) high edge shear, $s \equiv (r / q)(dq / dr)$, which is produced following the current ramp-down. Stability properties of TAE modes in high $\varepsilon\beta_p$ TFTR discharges are presently being studied [21,22].

4. Observation of current relaxation in high $\varepsilon\beta p$ discharges dominated by non-inductive currents

Due to the transient nature of the current profile modification that follows an I_p ramp-down, the enhanced stability created by the rapid current ramp-down deteriorates as the heating pulse length is extended. In order to investigate this effect further, high $\varepsilon\beta_p$ discharges were maintained for a constant-current relaxation time [23] by substantially reducing both the neutral beam power and the plasma current so that $\varepsilon\beta_p \sim 1$ while $\beta_N \leq 2$.

Figure 5 illustrates the time evolution of two long-pulse, high $\varepsilon\beta_p$ discharges. Figure 5a shows a discharge prepared with a 1.0 MA to 0.6 MA current ramp with 9 MW of neutral beam heating (5.5 MW co-injected and 3.5 MW counter-injected), and Figure 5b shows a discharge following a 0.85 MA to 0.4 MA current ramp with 8 MW of nearly balanced injection. As described in Refs. 1, 2, and 5, over 20 MW has been applied for short intervals producing $\beta_N > 4$ with high l_i. The discharges illustrated in Figure 5 represent the longest-lived high $\varepsilon\beta_p$ plasmas so far produced in TFTR. At 0.6 MA, a disruption terminated the discharge after 1.9 s of neutral beam heating at $\beta_N \sim 2$. At 0.4 MA, a mild beta collapse dominated by $m/n = 3/2$ oscillations occurred after only 0.5 s when $\beta_N \sim 2.5$; however, the 3/2 oscillations subsided and the discharge remained at $\varepsilon\beta_p \sim 1$ for an additional 2 s when it suffered a beta collapse at $\beta_N \sim 1.4$ associated with 3/1 oscillations. For both current levels, when the power was reduced so that $\beta_N < 1.1$, high amplitude MHD oscillations did not occur for the entire 4 s beam pulse; however, these plasmas had a relatively large surface voltage, and τ_E (and β_p)

gradually decayed to a low-current L-mode in a manner similar to that described in Ref. 13.

The current profiles following the current ramp were highly peaked, $l_i \geq 3$, and they evolved on a constant-current, resistive time scale to a relaxed state with a very small voltage throughout the plasma. Figure 6 shows the current and voltage profiles calculated by TRANSP at the beginning and end of each high $\varepsilon\beta_p$ discharge. The large negative surface voltage and the outer current reversal layer produced by the I_p ramp-down are indicated. After approximately 2 s, the measured surface voltages were less than 50 mV, and the TRANSP-calculated voltage profiles vanished except near the magnetic axis. The sum of the bootstrap and beam-driven currents were calculated to constitute approximately 90 % of the 0.6 MA discharge and more than 75% of the 0.4 MA discharge. Measurements of the $q(0)$ evolution using a motional Stark effect (MSE) diagnostic [24] were made during the first 2 s of each discharge, and the TRANSP calculations were in reasonably good agreement with the measurements of the 0.4 MA discharge. Work to better integrate the MSE measurements with TRANSP is in progress.

Ideal MHD stability analyses for $n = 1$ free-boundary modes were performed for the equilibria reconstructed by TRANSP at several times indicated in Figure 6 by either "S" or "U" (for stable or unstable). As shown, the appearance of MHD instabilities approximately corresponded to theoretical expectations. The equilibrium calculated to be unstable at 4.5 s in the 0.4 MA discharge could be stabilized by a slight reduction in the peak pressure. Although the initial plasma profiles were far from stability boundaries at the reduced power levels, as the profiles evolved, the calculated onset for $n = 1$ instabilities appears to describe operational stability limits of the high $\varepsilon\beta_p$, nearly steady-state discharges.

5. Summary

High l_i discharges have been produced with a rapid current ramp-down technique allowing supershot beta limits to be exceeded for short times in TFTR. For 1.0 MA discharges following a current ramp, the fusion reactivity can double relative to 1.0 MA supershots since the normalized beta limit was extended from approximately 2.0 to 3.5. The rapid current ramp did not prevent 1.0 MA discharges from achieving global energy confinement times comparable to supershots. The combination of improved stability with good confinement produced a second high Q_{DD} operate mode for TFTR.

The current profiles produced from the current ramps have not been maintained with current drive, and, consequently, high l_i, enhanced stability deteriorates as the pulse lengths are extended. Our observations of beta-limiting phenomena which occur after an I_p ramp-down are summarized in Figure 7. Enhanced stability relative to supershots has been observed for approximately 0.5 s. This is sufficiently long to allow the formation of $\langle\beta_\alpha\rangle >$

0.2 %. By reducing the injected power and operating at low current ($I_p \leq 0.6$ MA), high $\varepsilon\beta_p$ discharges with large fractions of non-inductive current have been sustained for a more than a current relaxation time.

References

[1] G. Navratil, *et al.*, *Plasma Phys. and Contr. Nuc. Fus.*, Vol. 1, (1990) 209.

[2] S. Sabbagh, *et al.*, *Phys. of Fluids B*, **2** (1991) 2277.

[3] K. McGuire, *et al.*, *Plasma Phys. Contr. Fusion* **30** (1988) 1391.

[4] J. Manickam, *et al.*, *Plasma Phys. and Contr. Nuc. Fus.*, Vol. 1, (1988) 395.

[5] M. E. Mauel, *et al.*, *Nuc. Fus.* **32** (1992) 1468.

[6] Y. Nagayama, *et al.*, submitted to *Phys. Rev. Letters.*

[7] T. S. Taylor, *et al.*, *Plasma Phys. and Contr. Nuc. Fus.*, Vol. 1, (1990) 177.

[8] J. Ferron, *et al.*, *Bull. Amer. Phys. Soc.* **36** (1991) 2324.

[9] M. G. Bell, *et al.*, *Plasma Phys. and Contr. Nuc. Fus.*, Vol. 1, (1988) 27.

[10] P. N. Yushmanov, *et al.*, *Nuc. Fus.* **30** (1990) 1999.

[11] M. C. Zarnstorff, *et al.*, Paper A-II-2, these proceedings.

[12] R. J. Goldston, *et al.*, *J. Comput. Phys.*, **43** (1981) 61.

[13] M. C. Zarnstorff, *et al.*, *Plasma Phys. and Contr. Nuc. Fus.*, Vol. 1, (1990) 183.

[14] H. Murmann, *et al.*, in *Proc. of 17th European Conf. on Contr. Fusion and Plasma Heating* Amsterdam (EPS, Petit-Lancy, Switzerland, 1990), Vol. 14B, Part I, p. 54.

[15] C. E. Bush, *et al.*, *Plasma Phys. and Contr. Nuc. Fus.*, Vol. 1, (1990) 309.

[16] C. E. Bush, *et al.*, "Characteristics of the TFTR limiter H-mode: the transistion, ELMs, transport, and confinement," submitted to *Nuc. Fus.*

[17] K. Toi, *et al.*, in *Contr. Fusion and Plasma Phys* (Proc. 16th Eur. Conf. Venice, 1989), Vol. 13B, Part I, EPS (1989) 221.

[18] J. Manickam, "External kink modes as a model for MHD activity associated with ELMs," PPPL Report No. 2819, Princeton University, January, 1992.

[19] B. Budny, *et al.*, *Nuc. Fus.* **32** (1992) 456.

[20] G. Y. Fu and C. Z. Cheng, *Phys. Fluids B*, **2** (1990) 985.

[21] C. Z. Cheng, *Phys. Fluids B*, **3** (1991) 2463.

[22] C. Z. Cheng, *et al.*, Paper D-II-1, these proceedings.

[23] D. R. Mikkelsen, *Phys. Fluids B*, **1** (1989) 333.

[24] F. Levinton, to be submitted to *Phys. Fluids B*.

Figure Captions

Figure 1. (a) Contours of the observed peak neutron rates as a function of plasma current for TFTR supershots and high $\varepsilon\beta_p$ discharges. (b) TFTR's operational diagram showing two high Q_{DD} operating regimes as a function of $\varepsilon\beta_p$ and the cylindrical safety factor, q^*.

Figure 2. The time evolution of high β_p discharges created with a 1.6 MA to 1.0 MA current ramp. Four discharges are superimposed to show the appearance of MHD limiting instabilities at lower values of β_N as time progresses.

Figure 3. Comparisons of the time evolution of (b) high $\varepsilon\beta_p$ discharges with (a) 1.0 MA and (c) 1.7 MA supershots. From top to bottom, the plasma current and the injected neutral beam power, the evolution of β_N, the DD fusion neutrons, the D_α light, and an estimate of the global energy confinement time.

Figure 4. (a) Calculated current profiles and total pressure parameters for the discharges shown in Figure 3. (b) Ideal $n = 1$ MHD instability thresholds calculated using $q(\psi)$ profiles approximating supershot and high l_i current profiles.

Figure 5. High $\varepsilon\beta_p$ discharges maintained for more than a constant-current relaxation time. From top to bottom, the injected beam power, the plasma current with calculated beam and bootstrap currents, the evolution of $\varepsilon\beta_p$, and the calculated values of l_i and $q(0)$. MSE measurements of $q(0)$ are superimposed onto the TRANSP calculated values.

Figure 6. The current and voltage profiles calculated by TRANSP for the discharges shown in Figure 5.

Figure 7. The observed onset of beta-limiting instabilities as a function of time after the end of a current ramp.

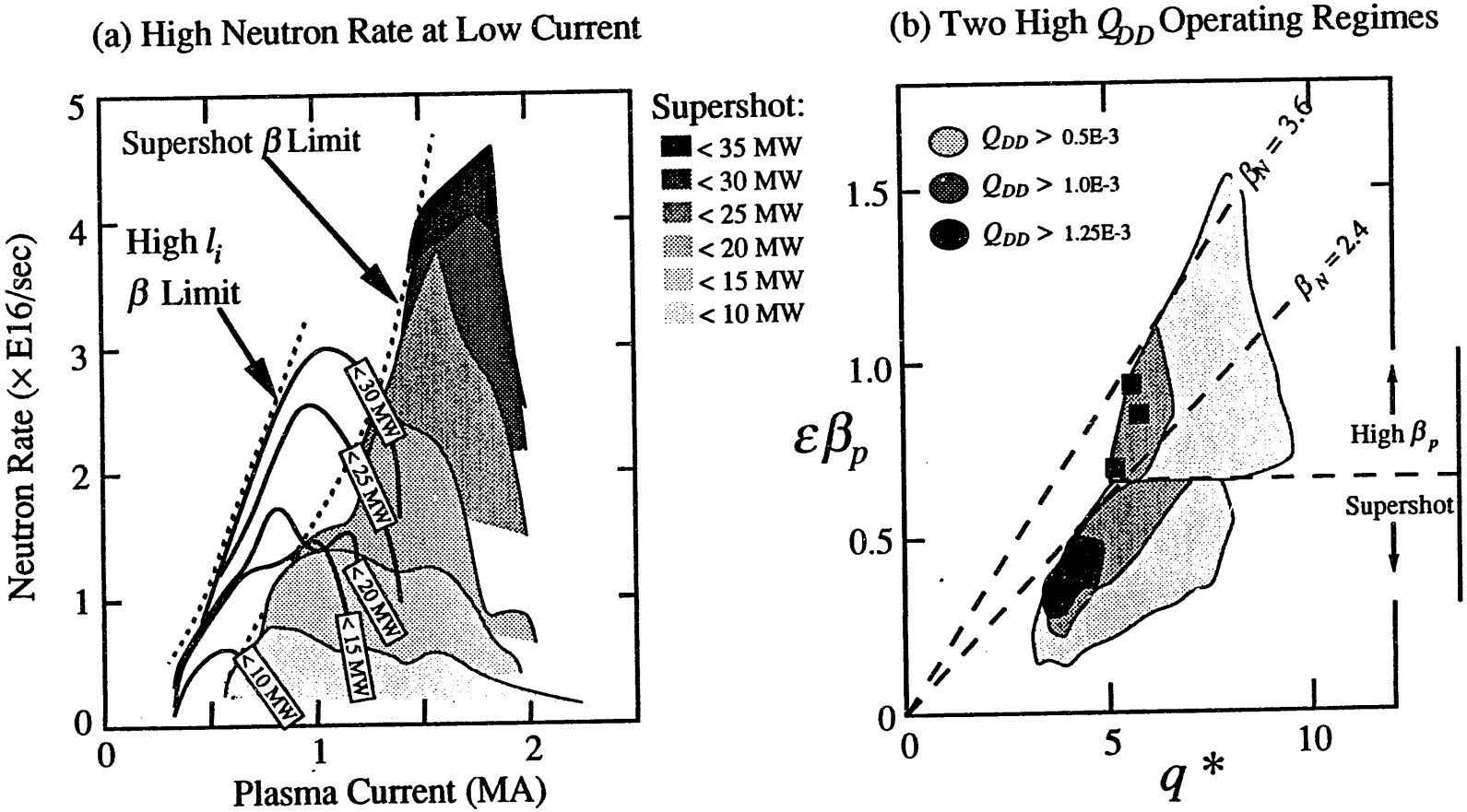
(a) High Neutron Rate at Low Current
Supershot β Limit
High l_i
β Limit
Supershot:
< 35 MW
< 30 MW
< 25 MW
< 20 MW
< 15 MW
< 10 MW
Neutron Rate (× E16/sec)
Plasma Current (MA)
(b) Two High Q_{DD} Operating Regimes
Q_{DD} > 0.5E-3
Q_{DD} > 1.0E-3
Q_{DD} > 1.25E-3
$\beta_N = 3.6$
$\beta_N = 2.4$
High β_p
Supershot
$\varepsilon\beta_p$
$q*$

Fig. 1

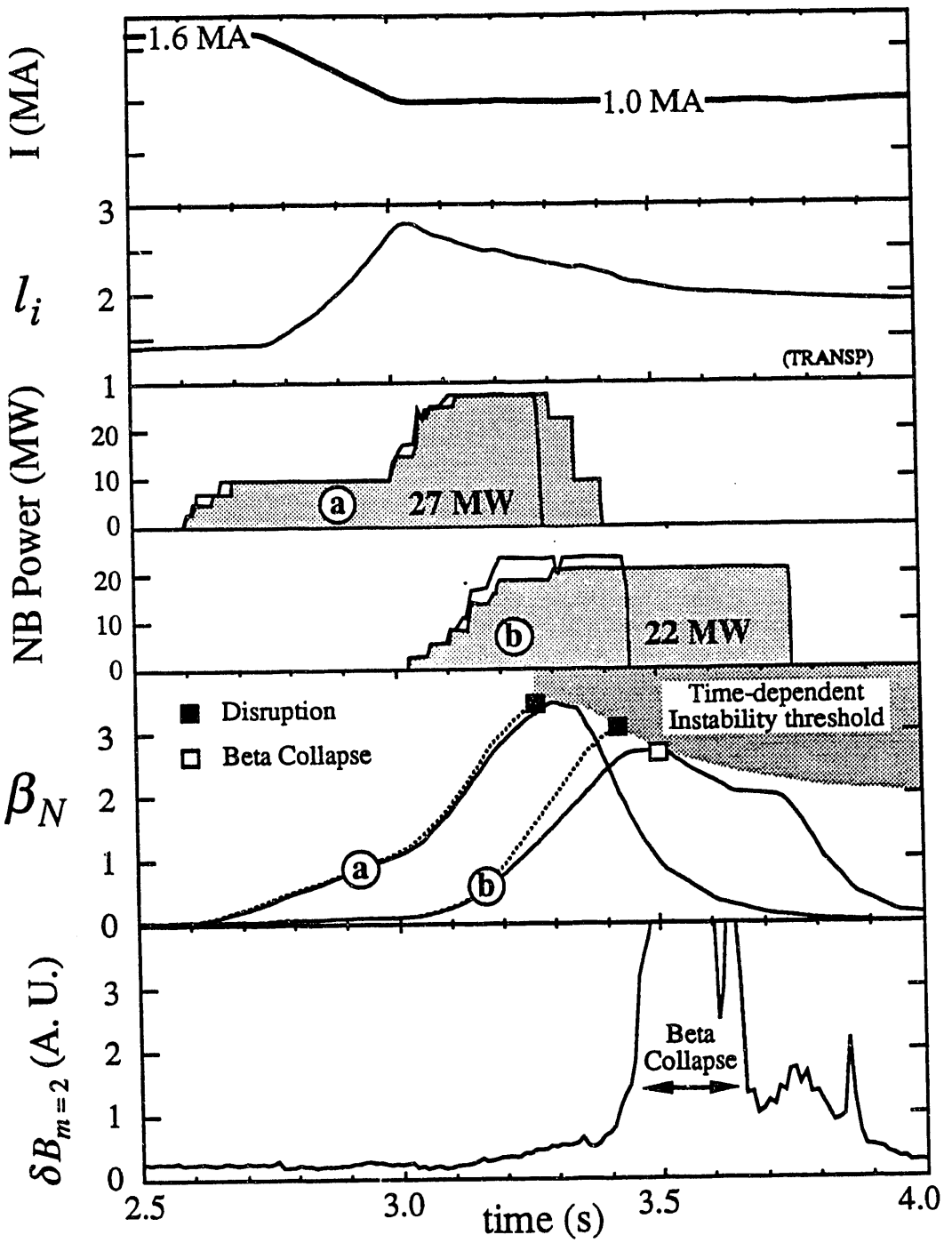
1.6 MA
1.0 MA
I (MA)
l_i
(TRANSP)
NB Power (MW)
27 MW
22 MW
Disruption
Beta Collapse
Time-dependent
Instability threshold
β_N
$\delta B_{m=2}$ (A. U.)
Beta
Collapse
time (s)

Fig. 2

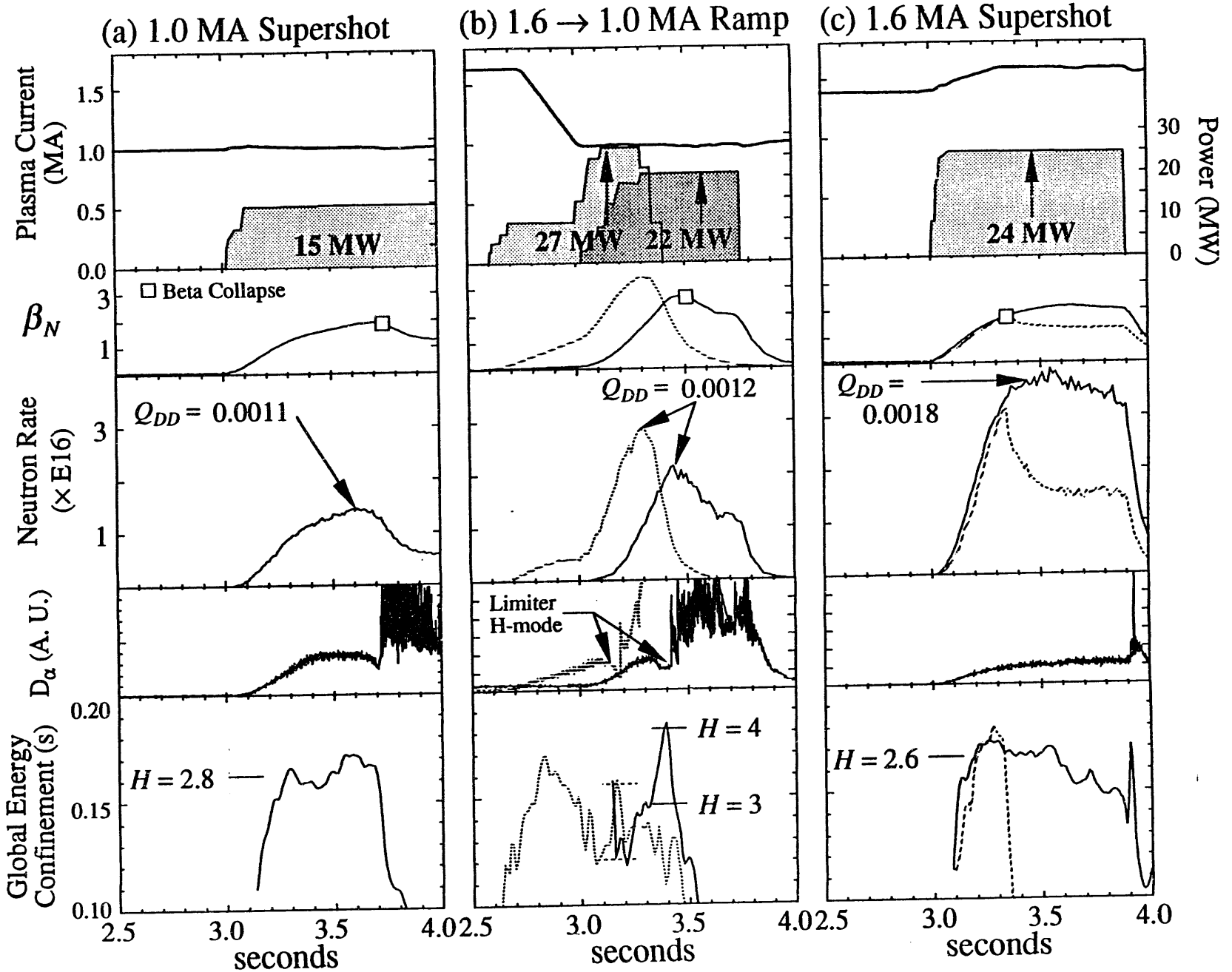
(a) 1.0 MA Supershot
(b) 1.6 → 1.0 MA Ramp
(c) 1.6 MA Supershot
Plasma Current (MA)
1.5
1.0
0.5
0.0
15 MW
27 MW
22 MW
24 MW
30
20
10
0
Power (MW)
Beta Collapse
β_N
3
1
Q_{DD} = 0.0011
Q_{DD} = 0.0012
Q_{DD} = 0.0018
Neutron Rate (× E16)
3
1
D_α (A. U.)
Limiter H-mode
Global Energy Confinement (s)
0.20
0.15
0.10
H = 2.8
H = 4
H = 3
H = 2.6
2.5
3.0
3.5
4.0
seconds

Fig. 3

(a) TRANSP Calculated $\langle J \rangle$ Profiles

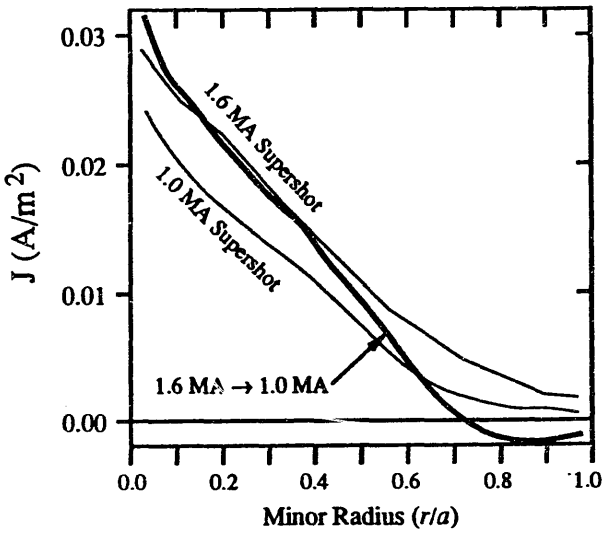

	$n_e(0)/\langle n_e \rangle$	$\langle p^2 \rangle / \langle p \rangle^2$
1.0 MA Supershot	3.0	2.35
1.0 MA *Ip* Ramp	2.4	2.05
1.6 MA Supershot	2.7	2.35

(b) Ideal $n = 1$ β limits for TFTR profiles

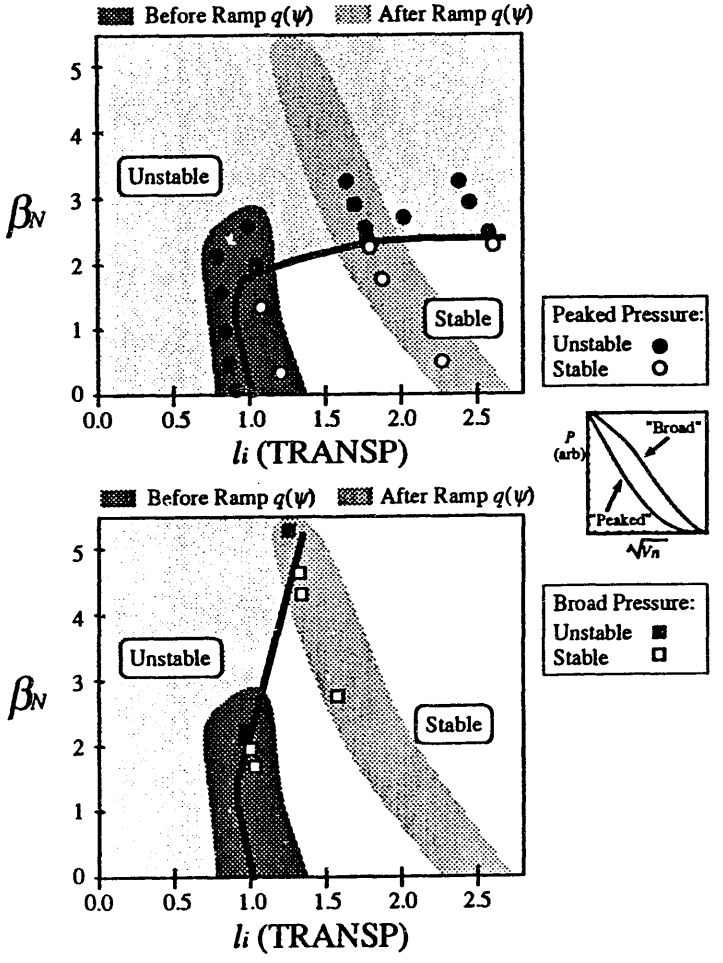

Fig. 4

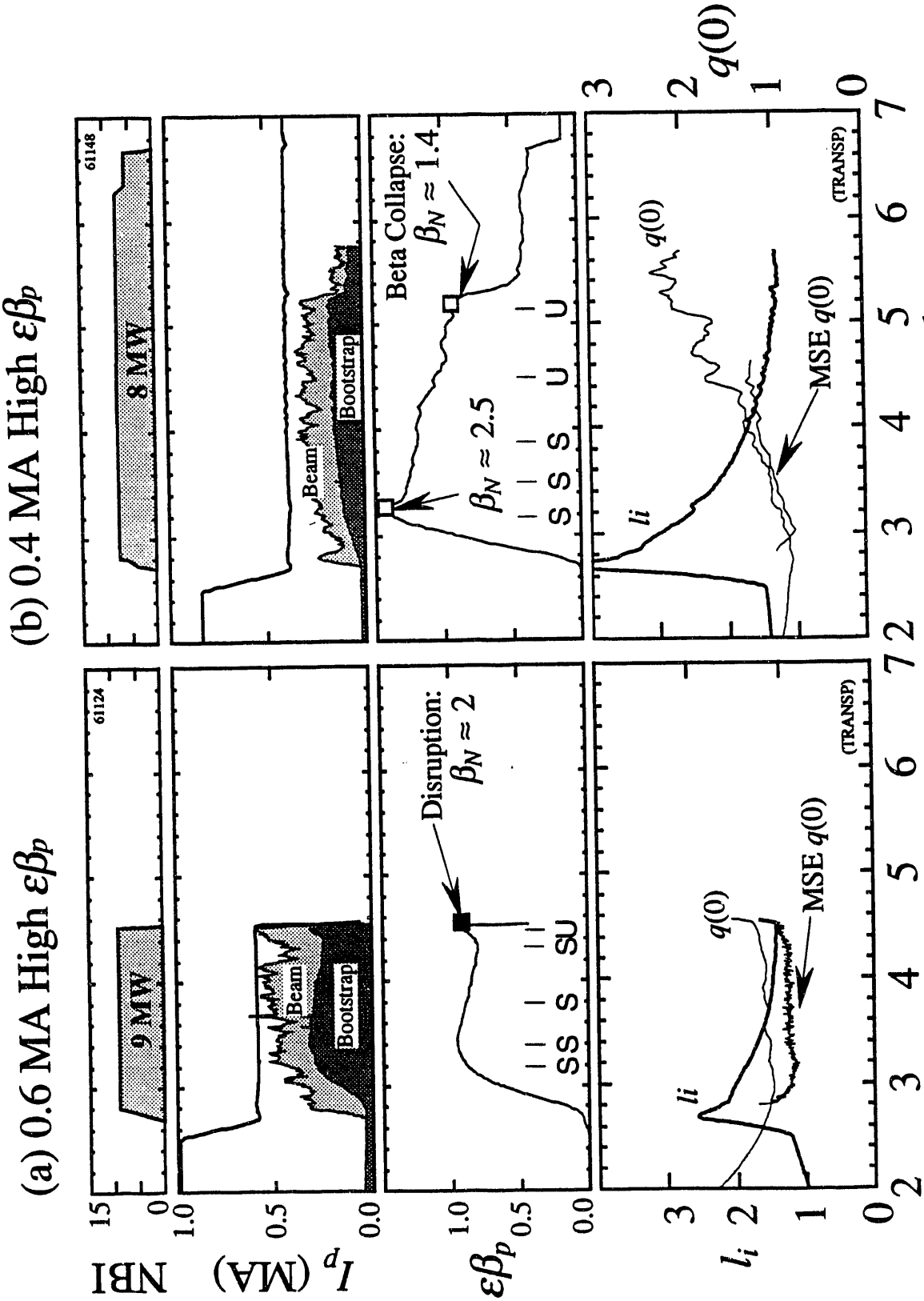
(a) 0.6 MA High $\varepsilon\beta_p$
(b) 0.4 MA High $\varepsilon\beta_p$
61124
61148
9 MW
8 MW
NBI
Beam
Bootstrap
I_p (MA)
$\varepsilon\beta_p$
Disruption: $\beta_N \approx 2$
Beta Collapse: $\beta_N \approx 1.4$
$\beta_N \approx 2.5$
S S S U U
S S S U
li
l_i
q(0)
MSE q(0)
(TRANSP)
Seconds

Fig. 5

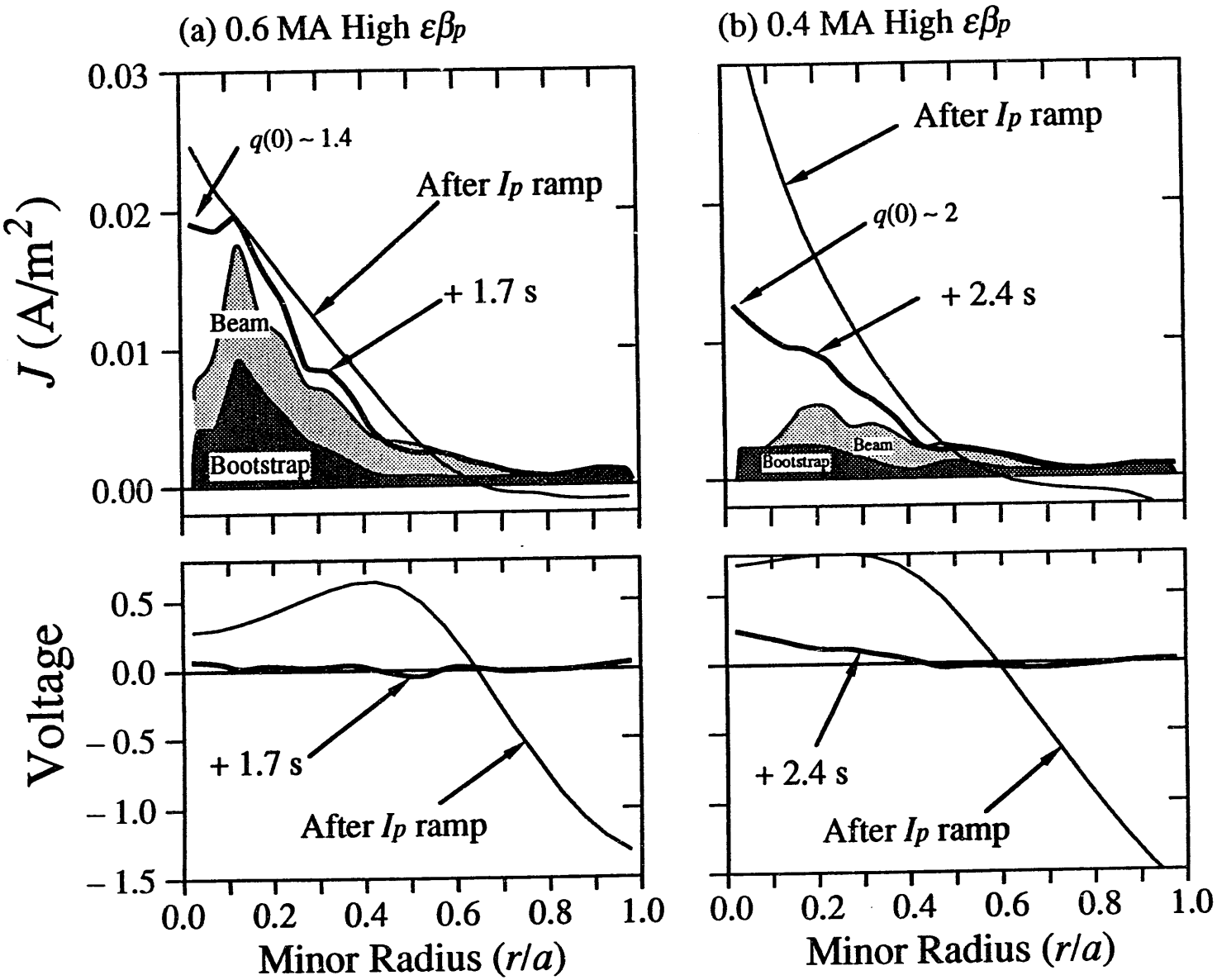
(a) 0.6 MA High $\varepsilon\beta_p$
(b) 0.4 MA High $\varepsilon\beta_p$
J (A/m^2)
0.03
0.02
0.01
0.00
$q(0) \sim 1.4$
After I_p ramp
+ 1.7 s
Beam
Bootstrap
$q(0) \sim 2$
+ 2.4 s
Voltage
0.5
0.0
−0.5
−1.0
−1.5
0.0
0.2
0.4
0.6
0.8
1.0
Minor Radius (r/a)

Fig. 6

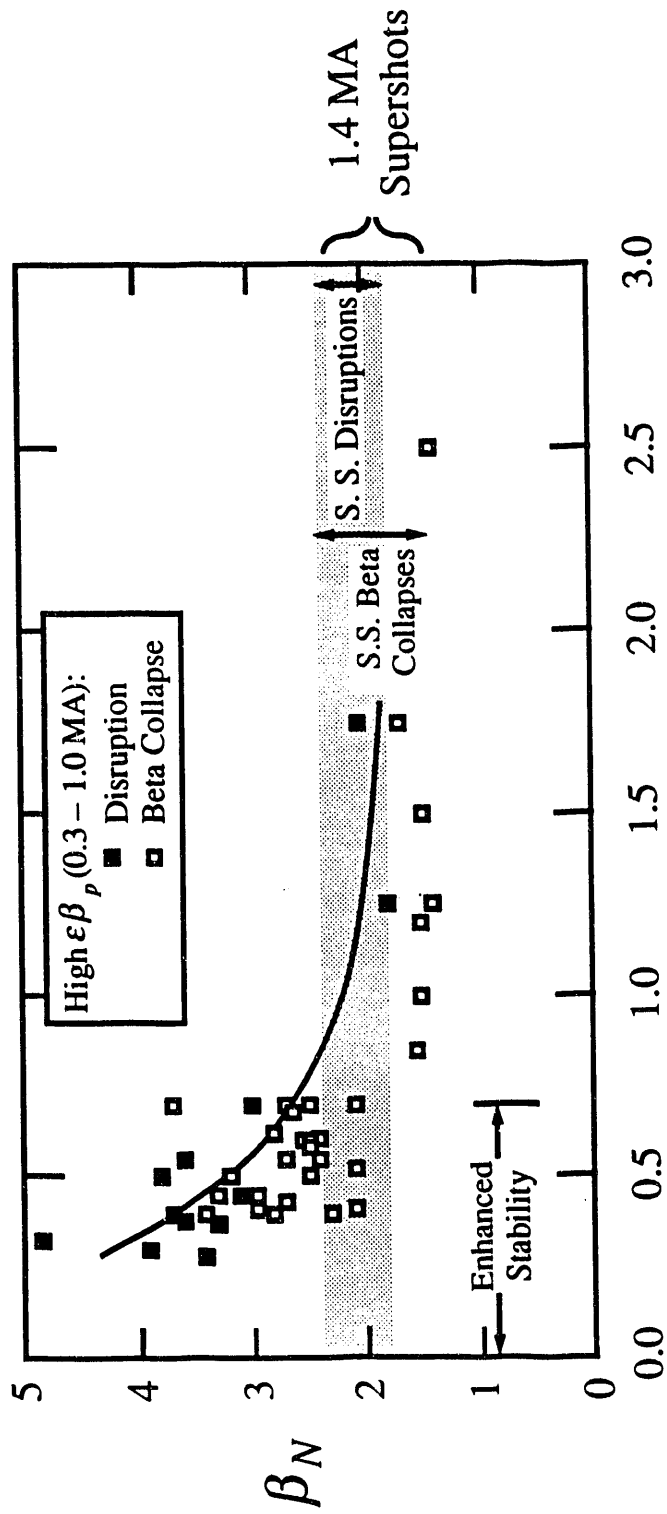
1.4 MA
Supershots
S. S. Disruptions
S.S. Beta
Collapses
High $\epsilon\beta_p$ (0.3 – 1.0 MA):
Disruption
Beta Collapse
Enhanced
Stability
β_N
Time after I_p Ramp (s)
0
1
2
3
4
5
0.0
0.5
1.0
1.5
2.0
2.5
3.0

Fig. 7

DATE
FILMED
7/12/93